Light-trapping in solar cells by photonic nanostructures: the need for benchmarking and fabrication assessments

Frank Lenzmann[1], Jyri Salpakari[1], Arthur Weeber[1], Carol Olson[1]
[1] ECN Solar Energy, P.O. Box 1, 1755 ZG Petten, The Netherlands

***Abstract* — Light-trapping in solar cells by photonic nanostructures, e.g., nano-textured surfaces or metallic and non-metallic nanoparticles is a research area of great promise. A large multitude of configurations is being explored and there is a rising need for (a set of) assessment elements that help to narrow in on the most viable ones. This paper discusses two examples: benchmark devices and the assessment of fabrication aspects for the nanostructures.**

***Index Terms* — light trapping, solar cells, nanostructures, benchmarking**

I. Introduction

Light-trapping is crucial in solar cells, in particular those based on amorphous and microcrystalline silicon thin films due to the unfavourable charge carrier mobilities and lifetimes in these materials. Also for crystalline silicon solar cells, the industry trend to decrease the thickness of the light-absorbing wafer to reduce material costs [1] accentuates the rising need for highly efficient light-trapping concepts.

State-of-the-art light-trapping concepts rely on random surface textures leading to efficient path length enhancement of the incident sunlight. These textures randomize the light propagation direction in the absorbing material which leads to total internal reflection. For such light-trapping schemes, the standard theory shows that the absorption enhancement factor has an upper limit of $4n^2/\sin^2\theta$, where n is the refractive index of the absorbing layer and θ is the angle of the emission cone in the medium surrounding the cell [2].

New light-trapping concepts based on photonic optics hold large promise in that the above specified limit of light-trapping can be surpassed by these approaches [2]. Photonic light-trapping is expected to enable extremely thin solar cells to achieve efficiencies rivalling or surpassing those of the thicker solar cells manufactured today (leading to cost savings).

Due to the relatively straightforward integration, the most abundantly explored configurations employ photonic structures at the front surface of solar cells (= side of light incidence). Numerous studies have been published in recent years documenting the enhanced light-trapping arising from such front-side photonic arrays in solar cells, e.g., [3]- [7]. It is important to note that these studies typically assess the enhanced light-trapping by comparison with reference devices that differ from the photonic solar cells only in the absence of the photonic structures. These reference devices are indeed most appropriate for scrutinizing the fundamental aspects of the associated photonic optics. However, they are in general configured without (optimized) conventional light-trapping schemes and thus don´t provide a comparison of the photonic concepts to state-of-the-art light-trapping benchmarks. The consequent inclusion of thorough benchmarks in future studies would therefore definitely be helpful in assessing the full value of the various photonic configurations.

Another quite characteristic aspect of many publications in the field of photonic light-trapping, is that they provide very little assessment of fabrication aspects for the nanostructures. This would be desirable though, because meeting the requirements for industrial processing in the photovoltaic industry, e.g., high throughput rates and relatively low complexity, is by no means evident.

II. Benchmarking of Photonic Light-Trapping Concepts

Figure 1 shows a sketch of three (thin-film a-Si:H) solar cells differing from each other only in their light-trapping schemes.

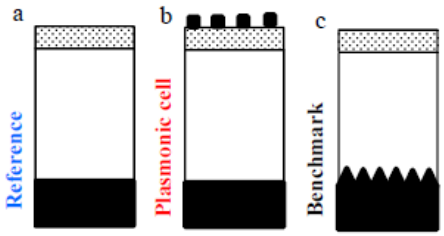

Fig. 1: Illustrations showing schematically the various thin layers of three different solar cells (a - c). These are (from bottom to top): a Ag/ZnO:Al back reflector layer (in black), an n-i-p a-Si:H stack (in white) and an ITO antireflection layer (dotted). Sample b comprises a plasmonic Ag nanocylinder array on top of the ITO layer (black squares). The back reflector layer is deposited on top of a flat glass substrate for samples a and b. For sample c it is deposited on top of a textured glass substrate (SnO_2 coated glass, "Asahi U", in which the texture is defined by the surface structure of the SnO_2 layer).

Cell b comprises a plasmonic Ag nanoparticle array at the front-side. Cell a serves as reference (which differs from plasmonic cell b only in the absence of the Ag nanoparticle array) and cell c is the benchmark device with a textured back-side reflector. The parameters in which the three cells differ from each other are summarized in table 1.

TABLE I: PARAMETRIZATION OF THE 3 SOLAR CELLS.

Solar cell	Plasmonic array	Substrate
a = Reference	No	Flat
b = Plasmonic cell	Yes	Flat
c = Benchmark (Asahi)	No	Textured

The plasmonic array of cell b consists Ag nano-cylinders with a diameter of 200 nm arranged in a square pattern of 450 nm pitch as shown in the SEM image of figure 2.

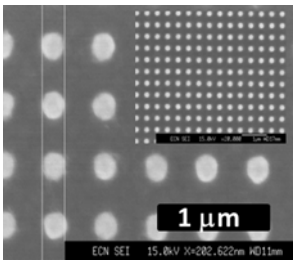

Fig. 2: SEM image of the plasmonic array consisting of Ag nano-cylinders on top of an a-Si;H solar cell.

In the inset of the SEM image a larger area of the plasmonic array is visible showing the perfect regularity of the pattern. The height of the cylinders is approximately 80 nm as determined by AFM measurements. This plasmonic design and an analysis of its (photo)electric function was recently published in [7].

Figure 3 depicts the external quantum efficiency of the three solar cells which show very different spectral fingerprints.

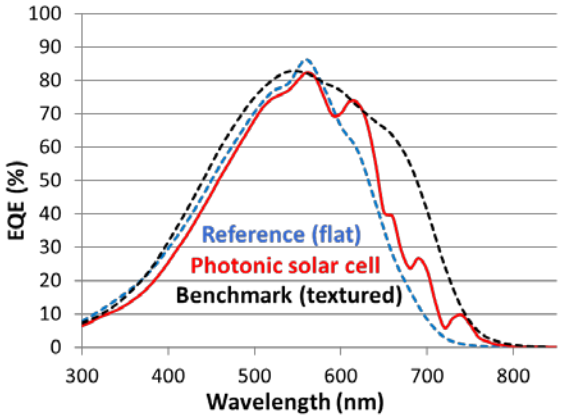

Fig. 3: EQE spectra of the four a-Si:H solar cells compared in this study. The characteristic differences in the spectral fingerprints are discussed in the text.

Compared to the flat reference cell (blue line), the plasmonic solar cell (red line) shows a clearly enhanced red response due to the presence of distinct peaks in the spectral range between 600 – 800 nm. These peaks rise well above the EQE values of the reference cell and can be assigned to the in-coupling of light to distinct waveguide modes of the thin a-Si:H layer as shown by us recently [7].

Compared to the textured benchmark cell (black line) however, the plasmonic cell shows significantly lower EQE values across the complete 300 - 800 nm wavelength range. Most importantly, in the range between 600 – 800 nm the benchmark device outperforms the plasmonic solar cell (very) clearly. Here the benchmark configuration shows a large and continuous broadband enhancement with respect to the planar reference device. The plasmonic device on the other hand shows distinct peaks most of which are also lower in intensity than the "envelope" defined by the benchmark response.

Within the boundary conditions of the described set of samples the coupling to distinct waveguide modes (in the plasmonic solar cell) clearly leads to a less effective enhancement of the total EQE than the random scattering of the benchmark. We note here, that improvements of the plasmonic array configuration are certainly possible as explained in more detail in [7]. Further optimizations of, e.g. diameter, height, pitch and location (e.g., front-side, rear-side) of the plasmonic arrays as well as the application of other materials (than Ag) are investigated by us in the frame of an on-going Dutch collaborative research initiative [8].

The purpose of this present paper however is not focussed on such improvements. Instead the purpose is to demonstrate with this example the importance of including a benchmark sample. This puts the performance of a given photonic light-trapping scheme into a broader perspective and allows in this way a maximally meaningful assessment of its full application potential..

III. ASSESSMENT OF FABRICATION ASPECTS

As indicated in the introduction, the application of photonic nanostructures in the PV industry ultimately requires that the processing of such structures complies with characteristic fabrication standards of this industry, such as high throughput rates and relatively low process complexity (in order to achieve low cost).

Throughput rate and process complexity

Typical throughput rates for wafer based silicon photovoltaics in current manufacturing lines are ≥ 3000 wafers/hour [7]. The International Technology Roadmap for Photovoltaics expects this value to increase up to ~ 7200 wafers/hour until 2020 [7]. Nanostructure fabrication techniques based on slow processing rates, like e.g. electron-beam lithography may therefore be very appropriate for the fabrication of complex nanostructures and in fundamental research but the current state of this technique offers no practical perspectives to be applied in the PV industry.

An example for a faster technique is nanoimprint lithography. Many variations of this technique are under development now which are capable of achieving accurate large area depositions and impressive throughput rates of up to 100 – 200 wafers/hour [9]. Further improvements can certainly be expected in this dynamically developing technology field.

The high throughput rates of the PV industry are – among other factors – a consequence of the requirement of low cost which is achieved by process flows with a relatively low complexity. Typical industrial p-type silicon solar cells are

processed following a sequence of only 9 major manufacturing steps [10]: (1) saw damage removal, texturing and cleaning of the silicon wafer, (2) Phosphorous diffusion, (3) Phosphorous glass removal and single-side etch for edge isolation, (4) Silicon nitride deposition, (5) Ag screen-printing and drying of front contacts, (6) Al/Ag screen printing and drying of rear busbars, (7) Al screen printing of rear, (8) Co-firing of front and rear contacts, (9) IV measurement and sorting.

For a nanofabrication technology to be viable for integration into such a "lean" process flow, a minimum of added process complexity - allowing to maintain a high throughput rate of the overall process flow at a minimum of added cost - is desirable. The processing via "temporary masks" - as typically required for example in imprint lithographic techniques - is a drawback in this respect. These masks are fabricated in a sequence of 3 processing steps [11]: (1) deposition of the imprint resist layer onto the surface to be endowed with the nanopattern (2) imprinting by means of a stamp applied to the imprint resist layer, curing and stamp release (3) removal of the "residual layer" (very thin layer of imprint resist systematically remaining on the surface in areas where the imprint resist layer is ultimately intended to be completely removed).

In particular, the resist spread time associated with step 2 has been identified as the primary throughput-limiting factor for nanoimprint lithography [9]. For the fabrication of the Ag nano-cylinder arrays described in section II of this paper two more steps are then still required after the fabrication of the mask. These steps are (4) evaporation of Ag, and (5) stripping of the mask. We note here, that several (or all) of the steps described above may be advantageously integrated into one single fabrication tool.

Including critical discussions like above of fabrication technologies as part of a more harmonized set of assessment criteria in the area of photonic light-trapping for solar cells can be of large added value for the identification of the most urgent development needs. In particular, the specification of current (and the estimation of future) throughput rates will certainly be very helpful.

IV. Conclusions

This paper addressed the issue of finding a good set of assessment elements in the research field of light-trapping for solar cells by photonic nanostructures. In order to show the full potential and industrialization perspectives of the existing multitude of configurations, we conclude that the following two elements should be included as a minimum: (1) benchmark devices representing optimized state-of-the-art conventional light-trapping schemes, and (2) critical discussions of fabrication technologies addressing in particular the throughput (perspectives) of a given fabrication technology in comparison with the throughput standards of the PV industry.

Acknowledgement

This work has been supported by the Dutch NanoNextNL program under the program 2A.

References

[1] International technology roadmap for photovoltaics. SEMI PV Group, http://www.itrpv.net, 2012.

[2] Z. Yu, A. Raman, and S. Fan, "Fundamental limit of nanophotonic light trapping in solar cells", *PNAS*, vol. 107/ 41, p. 17495, 2010.

[3] D. Derkacs, S.H. Lim, P. Matheu, W. Mar, and E.T. Yu, "Improved performance of amorphous silicon solar cells via scattering from surface plasmon polaritons", *Appl. Phys. Let., vol.* 89/9, p. 093103, 2006.

[4] S. Pillai, K.R. Catchpole, T. Trupke, and M.A. Green, "Surface plasmon enhanced silicon solar cells", *J. Appl. Phys.*, vol. 101/9, p. 093105, 2007.

[5] P. Matheu, S.H. Lim, D. Derkacs, C. McPheeters, and E.T. Yu," Metal and dielectric nanoparticle scattering for improved optical absorption in photovoltaic devices", *Appl. Phys. Let.* vol. 93/11, p. 113108, 2008.

[6] P. Spinelli, M. Hebbink, R. de Waele, L. Black, F. Lenzmann, and A. Polman, "Optical impedance matching using coupled plasmonic nanoparticle arrays", *Nano Lett.* vol. 11, p. 1760, 2011.

[7] M. van Lare, F. Lenzmann, M.A. Verschuuren, and A. Polman, "Mode coupling by plasmonic surface scatterers in thin-film silicon solar cells", *Appl. Phys. Lett.*, vol. 101, p. 221110 1-4, 2012.

[8] http://www.nanonextnl.nl/themes/energy/efficient-generation-of-sustainable-energy.html

[9] M. Malloy, L.C. Litt, "Technology review and assessment of nanoimpring lithography for semiconductor and patterned media manufacturing",*J. Micro/Nanolith. MEMS MOEMS*, vol. 10(3), p. 032001, 2011

[10] D.H. Neuhaus and A. Münzer, "Industrial SiliconWafer Solar Cells", *Advances in OptoElectronics*, vol. 2007, Article ID 24521, 2007.

[11] M. Verschuuren and R. Ji. "Full field nano imprint on mask aligners using substrate conformal imprint lithography technique", Technical report, SUSS MicroTec, 2009.